Xiaohua Liu
Aeroengine Airworthiness Certification Center
Preparatory Office,
China Academy of Civil Aviation
Science and Technology,
School of Energy and Power Engineering,
Beihang University,
No. 37 Xueyuan Road,
Haidian District, Beijing 100191, China
e-mail: Liuxh@sjp.buaa.edu.cn

Dakun Sun
School of Energy and Power Engineering,
Beihang University,
No. 37 Xueyuan Road,
Haidian District, Beijing 100191, China
e-mail: renshengming@sjp.buaa.edu.cn

Xiaofeng Sun
School of Energy and Power Engineering,
Beihang University,
No. 37 Xueyuan Road,
Haidian District, Beijing 100191, China
e-mail: Sunxf@buaa.edu.cn

Basic Studies of Flow-Instability Inception in Axial Compressors Using Eigenvalue Method

This paper applies a theoretical model developed recently to calculate the flow-instability inception of an axial transonic single stage compressor. After several calculation methods are compared, the singular value decomposition method is adopted to solve the resultant eigenvalue problem in which the involved matrix is rather large due to multistage configuration. The onset point of flow instability is judged by the imaginary part of the resultant eigenvalue. The effect of flow compressibility on the stall onset point calculation for the transonic rotor is studied. It is shown that the compressibility of flow perturbation plays a major role in computing high speed compressor flow stability.
[DOI: 10.1115/1.4026417]

Introduction

Flow instability is one of the severest challenges in turbomachinery. As one major type, rotating stall is a natural limit to the performance of compressors, which could cause catastrophic damage to the whole compression system. Considerable work was done during the past decades on investigating this phenomenon. Since the first explanation was given by Emmons [1] in 1955, much progress has been made by two different types of research approach.

The first type of approaches, analytical models, mostly focuses on the stall inception of turbomachinery in a simplified structure, and then solves an eigenvalue problem which is based on a small perturbation theory and mode decomposition technique. Nenni and Ludwig's work [2] resulted in an analytical expression for the inception condition of a two-dimensional incompressible rotating stall. Moore and Greitzer [3] presented a stability model of a compression system by a different approach. The model cannot only be used to predict the inception condition of stall and surge but also to study the nonlinear development of stall cells. Stenning [4] also studied the rotating stall based on a linearized small perturbation analysis in 1980. It is verified that all these analytical models can predict the instability inception condition with a satisfactory accuracy as long as sufficient loss and performance characteristics of the concerned compressors are available. Gordon [5] presented a three-dimensional (3D) incompressible stability model in annular domain. In recent years more attention is placed on the compressible flow stability in multistage compressors. Sun [6] and Liu et al. [7] developed two different kinds of three-dimensional compressible stability models including the effect of one novel casing treatment. It is found that the resultant criterion on the system stability using an analytical model is unambiguous. The second type of approach, numerical calculation, is developed rapidly nowadays. This method is to directly solve an unsteady Euler or Navier–Stokes equation as an initial boundary value problem to obtain the information related to the inception condition [8–14]. Escuret and Garnier [8], Longley [9], and Chima [10] applied different body force approaches to represent the effects of blades on the flow field and simulated the onset of rotating stall. Gong et al. [11] made the first effort to simulate three-dimensional nonlinear flow instability using a body force model. Hoying et al. [12], Vo et al. [13], and Chen et al. [14] performed computational study to investigate the stalling process. The advantage is that numerical calculation can consider the effects of more aerodynamic and geometrical parameters involved in the physical phenomena than analytical models.

On the one hand, for analytical models, the rotors and stators are simplified as a series of actuator disks or semiactuator disks. Two necessary assumptions are made as the mean flow is uniform and the characteristics data are already known. The effects of three-dimensional blade shape and flow details in passages cannot be directly and clearly included in these models. Plenty of simplification in these models weakens the possibility of making an instructive conclusion for blade optimization design. Furthermore, the prediction result using these models depends on the accuracy of the performance characteristics of compressors, which are not generally available with enough accuracy. Numerous requirements for the flow loss or flow angles restrict the practical application of analytical models, especially during the design stage of a new compressor without sufficient empirical correlations. On the other hand, as an initial boundary value problem, how and when the initial perturbation is introduced appropriately are essential issues faced by numerical calculation. Up to now, there have not been any rules and reliable evidence for overcoming this challenge. In addition, because different time and scale scales are involved in the rotating stall, the unsteady CFD method is unacceptable for industrial applications in terms of unsustainable computational source consumption. In conclusion, although a great deal of progress has been made on the mechanism of flow stability, little research has been conducted on the instability inception of compressible flow, including the effects of complex configuration of compressors. Furthermore, the shock wave embedded in cascade passages, which plays a vital role in flow field, introduces great difficulty in modeling the compressors system. Sun et al. [15] recently developed a new flow instability inception model by using an eigenvalue theory, and the computed stall onset point agrees well with the experimental results on both the low speed

Contributed by the Fluids Engineering Division of ASME for publication in the Journal of Fluids Engineering. Manuscript received June 15, 2013; final manuscript received December 23, 2013; published online January 27, 2014. Assoc. Editor: Zvi Rusak.

single rotor and the transonic single rotor. However, a rather large scale matrix due to multistage compressors, which is involved in the established eigenvalue equation, will not make the mathematical solution straightforward.

As far as the authors know, little research has been conducted on the stall inception prediction of transonic flow with general multiblade rows or single stage compressor configuration. Tryfonidis et al. [16] conducted an experimental investigation on eight different high speed compressors to study stall precursors using identical processing and detected the compressible mode and incompressible mode. Bonnaure [17] developed a two-dimensional (2D) compressible analysis for multistage compressors and showed a major effect of compressibility on the flow stability inception. But most existing analytical models are not established for compressible flow. In conclusion, a theoretical study, which can quantitively study the effect of flow compressibility on the stall inception prediction, remains some way off. It is the lack of such a study that motivated us to use our model for further investigation. The main purposes of this study are summarized as follows:

(1) To present several different calculation methods in order to select an effective mathematical solution in terms of accuracy and efficiency.
(2) To validate the feasibility of calculating the stall onset point for the transonic single stage compressor using the present flow stability model.
(3) To study the effect of the compressibility of flow perturbation on the stall onset point calculation for high speed compressors.

First, this model is outlined for completeness of this paper. Model assessment is performed on NASA stage 35 and the results verify that this model is capable of predicting the stall onset point of transonic compressors flow with reasonable accuracy and acceptable computational cost. Then the comparison of the computed stall onset points of one transonic rotor using both compressible and incompressible models shows the effect of flow perturbation compressibility on the instability inception prediction for transonic flow.

Stall Inception Model

A single stage compressor system, which consists of an inlet duct, blade rows region, interbladed row region, and an outlet duct, is shown in Fig. 1. In this paper the circumferentially averaged mean flow field and its derivative in the axial and radial direction are derived from steady computational fluid dynamics (CFD) which is performed by solving a routine 3D RANS equations solver. Then a flow model for studying the stability of small perturbation in compressor flow is required.

In this work, the action of blades on the flow field is represented by body force distributions and the viscosity outside the blade surface is neglected. The flow field is described by 3D, unsteady, compressible Euler equations with force source terms in a fixed frame of the coordinate system:

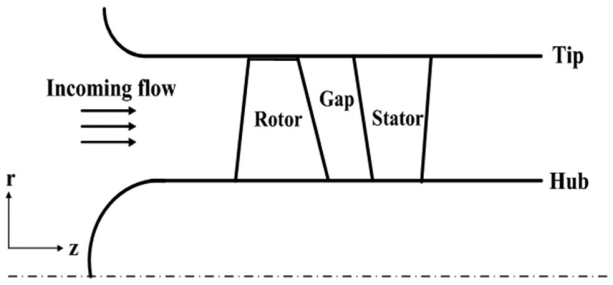

Fig. 1 Sketch of one stage compressor on the meridian plane

$$\frac{\partial \rho}{\partial t}+\frac{\partial(r\rho v_r)}{r\partial r}+\frac{\partial(\rho v_\theta)}{r\partial\theta}+\frac{\partial(\rho v_z)}{\partial z}=0 \tag{1}$$

$$\frac{\partial v_r}{\partial t}+v_r\frac{\partial v_r}{\partial r}+v_\theta\frac{\partial v_r}{r\partial\theta}+v_z\frac{\partial v_r}{\partial z}-\frac{v_\theta v_\theta}{r}=-\frac{1}{\rho}\frac{\partial p}{\partial r}+F_r \tag{2}$$

$$\frac{\partial v_\theta}{\partial t}+v_r\frac{\partial v_\theta}{\partial r}+v_\theta\frac{\partial v_\theta}{r\partial\theta}+v_z\frac{\partial v_\theta}{\partial z}+\frac{v_\theta v_r}{r}=-\frac{1}{\rho}\frac{\partial p}{r\partial\theta}+F_\theta \tag{3}$$

$$\frac{\partial v_z}{\partial t}+v_r\frac{\partial v_z}{\partial r}+v_\theta\frac{\partial v_z}{r\partial\theta}+v_z\frac{\partial v_z}{\partial z}=-\frac{1}{\rho}\frac{\partial p}{\partial z}+F_z \tag{4}$$

$$\frac{\partial T}{\partial t}+v_r\frac{\partial T}{\partial r}+v_\theta\frac{\partial T}{r\partial\theta}+v_z\frac{\partial T}{\partial z}+\frac{R}{c_v}T\left[\frac{\partial(rv_r)}{r\partial r}+\frac{\partial v_\theta}{r\partial\theta}+\frac{\partial v_z}{\partial z}\right]=0 \tag{5}$$

where the ideal gas law assumption is made to obtain the energy equation. Since emphasis is placed on the inception period of flow instability, the flow field is assumed to consist of mean flow and small disturbance

$$\vec{V}=\overline{V}+v' \tag{6}$$

$$p=\bar{p}+p' \tag{7}$$

$$\rho=\bar{\rho}+\rho' \tag{8}$$

$$F=\bar{F}+F' \tag{9}$$

where the overbar represents the mean flow and superscript prime represents the flow disturbance. After Eqs. (6)–(9) are substituted into Eqs. (1)–(5), the linearized N–S equations are derived. Furthermore, the small perturbation of flow field is assumed to be in the form of harmonic decomposition

$$\rho'=\tilde{\rho}(r,z)e^{i(-\omega t+m\theta)} \tag{10}$$

$$v_r'=\tilde{v}_r(r,z)e^{i(-\omega t+m\theta)} \tag{11}$$

$$v_\theta'=\tilde{v}_\theta(r,z)e^{i(-\omega t+m\theta)} \tag{12}$$

$$v_z'=\tilde{v}_z(r,z)e^{i(-\omega t+m\theta)} \tag{13}$$

$$p'=\tilde{p}(r,z)e^{i(-\omega t+m\theta)} \tag{14}$$

where the overtilde represents the amplitude of flow perturbations. Gordon [5] and He [18] demonstrated that higher order modes were usually more stable than lower order modes. Emphasis in this paper is therefore placed on the lowest order circumferential and radial mode which dominates the stability of the compressors system.

Many researchers have made considerable progress [19–22] on flow separation and stall prediction of airfoil. Rusak and Morris [23] successfully developed an asymptotic approach for providing a general criterion to determine the stall angle of leading-edge stall onset on thin airfoils at moderately high Reynolds number flows. This work can consider the effects of the airfoil's thickness ratio, nose radius of curvature, flow compressibility, camber, and flaps on the airfoil stall onset. Such an approach could be applied as a useful tool in the design of modern airfoils and wings. In 1955 Emmons [1] has given some physical explanation based on flow separation of the blade airfoil. It is doubtless that the investigation on the rotating stall of the compressors could benefit from the study on airfoil flow instability. Especially, it may be a good way to consider more flow details on compressor blades using an asymptotic approach. However, as stated by Sun et al. [15], the stalling process of compressors is related to not only the sudden flow separation and loss of lift on the blades but also the interactive effects of adjacent blade rows and the propagation of flow disturbance around the annulus. Therefore, many flow details on the cascade have to be neglected in the rotating stall inception model. An alternative and simplified approach is required. In order to make the complicated problem computationally feasible,

a body force approach is taken to consider the effects of blades on flow field. Theoretically, the present model can consider the flow details around the blade surface as long as the body force is accurately formulated. However, it will be a very complicated expression of detailed flow parameter and establishing the resultant eigenvalue equation will be very tricky. The body force model presented in this paper is a simplified approach to consider the main effects of blades on flow field.

There is no unified mathematic expression for body force. In addition, different sorts of body force models developed by Longley [9], Chima [10], and Gong et al. [11] perform well in reproducing the flow detail in blade passages provided that the conservation relations for mass, momentum, and energy are reflected correctly. In the present work a body force model F is applied as [24], which consists of two parts F_v and F_t. Figure 2 shows the components of body force. F_t, which is parallel to the camber surface and streamline, is mainly caused by viscosity on the blade surface. F_v is normal to the mean camber line of the blades in the blade-to-blade surface. The radial component of total body force is assumed to be negligible due to the small radial inclination of blades in this paper. Xu [25] conducted a rigorous study to assess viscous body forces for unsteady calculations and presented a simplified formulation to model the viscous force. The result verified that the viscous force is relatively small compared to the total blade forces. Therefore, F_t is assumed to be negligible in this paper. Furthermore, F_v is divided into two subparts: F_{v1} which is designed to contribute the work done by blades and F_{v2} which generates the flow loss of kinetic energy caused by circumferentially flow nonuniformity within the blade passages. It is noted that the applicability of the following linearization process and this simplified body force approach for reflecting the principle physical nature will ensure the reasonable accuracy for the prediction of the stall onset point during the model assessment part.

Based on the theorem of axial moment of momentum in turbomachinery, while the blades turn the relative flow toward the blade camber line, the work is done and the relative flow kinetic energy is transformed to the static pressure rise. The flow resistance is assumed to be zero since the viscosity is neglected. Therefore $F_{v1\theta}$, which is the circumferential component of F_{v1}, generates the flow turning. In steady, circumferentially averaged, three-dimensional flow field, the circumferential component of body force is described by the formula below:

$$F_{v1\theta} = v_r \frac{\partial v_\theta}{\partial r} + v_z \frac{\partial v_\theta}{\partial z} + \frac{v_\theta v_r}{r} \tag{15}$$

Meanwhile, in steady circumferentially averaged 2D flow field, F_θ is formulated as

$$F_{v1\theta} = v_z \frac{\partial v_\theta}{\partial z} \tag{16}$$

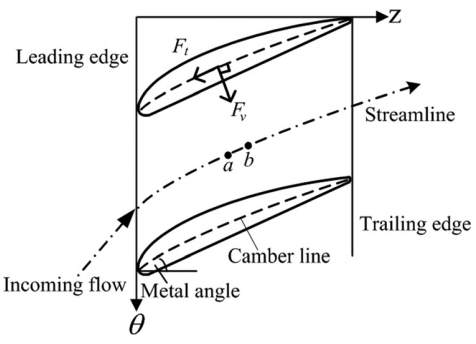

Fig. 2 Sketch of body force in blade-to-blade surface and two points (*a* and *b*) on one streamline

which is derived from the circumferential momentum equation. In accordance with Gordon's work [12], $F_{v1\theta}$ is assumed to turn the relative flow toward the blade angle, i.e.,

$$F_{v1\theta} = k_c v_z [v_z \tan\beta - (v_\theta - r\Omega) + \varepsilon] \tag{17}$$

The body force coefficient $k_c(r, z)$ is therefore determined by arranging Eqs. (15) and (17):

$$k_c = \frac{v_r \dfrac{\partial v_\theta}{\partial r} + v_z \dfrac{\partial v_\theta}{\partial z} + \dfrac{v_\theta v_r}{r}}{v_z [v_z \tan\beta - (v_\theta - r\Omega) + \varepsilon]} \tag{18}$$

where ε is a parameter which is large enough to avoid the singularity of k_c due to extreme small deviation angle of flow streamline. Theoretically, F_{v1} can only generate a circumferentially uniform flow field. However, the stability of a circumferential averaged flow field is studied in the present investigation. Thus, $F_{v2\theta}$, which is the circumferential component of F_{v2}, is designed to generate the flow loss of kinetic energy caused by the effects of flow nonuniformity and shock wave within blade passages on the meridian plane. The stagnation pressure and rotary stagnation pressure are defined as

$$p_t = p\left\{1 + \frac{\gamma - 1}{2}\frac{\rho[V_z^2 + V_r^2 + V_\theta^2]}{\gamma p}\right\}^{\frac{\gamma}{\gamma-1}} \tag{19}$$

$$\bar{p}_t = p_t - \rho\Omega r V_\theta \tag{20}$$

Rotary stagnation pressure, which represents for the total energy of rotating flow, will decreases along the streamline. If two points (a and b) lie on one streamline within the blade passage on the meridian plane of compressors, $F_{v2\theta}$ is assumed to be proportional to the rotary stagnation pressure drop within unit length along the streamline:

$$\rho F_{v\theta 2} \propto \frac{(\bar{p}_t)_b - (\bar{p}_t)_a}{(s_b - s_a)} \tag{21}$$

where s is the streamline coordinate and points a and b are very close:

$$s_b - s_a \approx \sqrt{(r_b - r_a)^2 + (z_b - z_a)^2} \tag{22}$$

In addition, the flow energy loss across the rotors and stators is assumed to be proportional to the local relative dynamic pressure. The loss coefficient is defined as

$$\lambda = \frac{(\bar{p}_t)_b - (\bar{p}_t)_a}{\rho\left[v_z^2 + (v_\theta - \Omega r)^2\right]_a} \tag{23}$$

Therefore $F_{v2\theta}$ can be formulated as follows by manipulating Eqs. (22) and (23):

$$F_{v2\theta} = \lambda \frac{\left[v_z^2 + (v_\theta - \Omega r)^2\right]}{r_b\theta_b - r_a\theta_a} \tag{24}$$

Finally the circumferential component of body force is given by Eqs. (17) and (24):

$$F_{v\theta} = F_{v1\theta} + F_{v2\theta} \tag{25}$$

Considering the orthogonality between body force and blade camber surface, the axial component F_z can be obtained directly:

$$F_z = -F_\theta \tan\beta \tag{26}$$

where β is the circumferential metal angle of blades and can be computed directly using the geometry data of the mean camber surface of blades.

It is noted that the strong discontinuity brought by a passage shock wave is eliminated in the meridian mean flow field. Therefore, the present model provides a possibility to deal with the stall margin prediction for transonic flow. As similar as Gordon's work [5], the unsteady action of blades on flow field is described by the body force function which responds to the local unsteady 3D flow variations in the blade region and the unsteady force disturbances f_θ and f_z are modeled by a first-order lag equation with a time delay constant τ. The linearized form of body force is formulated as

$$(1 - i\omega\tau + im\Omega\tau)f_\theta = \frac{\partial F_\theta}{\partial v_\theta}v'_\theta + \frac{\partial F_\theta}{\partial v_z}v'_z \tag{27}$$

$$(1 - i\omega\tau + im\Omega\tau)f_z = \frac{\partial F_z}{\partial v_\theta}v'_\theta + \frac{\partial F_z}{\partial v_z}v'_z \tag{28}$$

The time delay constant τ, which represents the lag between the output response and input data, is employed to describe the unsteady performance of compressors. The time scale of τ is generally assumed to be of the order of flow-through time in the bladed region. After Eqs. (10)–(14) and Eqs. (27) and (28) are substituted into Eqs. (1)–(5), the linearized governing equations are derived as

$$(\boldsymbol{A}D_r + \boldsymbol{B}D_z + \boldsymbol{C} - i\omega\boldsymbol{G})\Phi = 0 \tag{29}$$

where $\boldsymbol{A}$ is the radial derivative matrix and $\boldsymbol{B}$ is the axial derivative matrix. The boundaries are prescribed so that there are no inlet disturbances coming from outside of the system at the upstream end of the duct and no reflection at the downstream end of the duct, and the slip condition is used at the hub and tip of the annular duct. Since Eq. (29) is homogeneous, a nontrivial solution of $\boldsymbol{\Phi}$ exists only if the determinant of the coefficients matrix is zero, i.e.,

$$\det[\boldsymbol{X}] = 0 \tag{30}$$

$$\boldsymbol{X} = \boldsymbol{A}D_r + \boldsymbol{B}D_z + \boldsymbol{C} - i\omega\boldsymbol{G} \tag{31}$$

Solving the established eigenvalue problem Eq. (30) leads to the resultant complex frequency $\omega = \omega_r + i\omega_i$, the imaginary part of which represents whether the system is stable with negative value or unstable with positive value, and the real part of which determines the rotating frequency of the precursor wave. Two-nondimensional factors are defined as relative speed (RS) and damping factor (DF):

$$RS = \frac{\omega_r}{2m\pi} \cdot \frac{60}{\Omega} \tag{32}$$

$$DF = \frac{r_t\omega_i}{mU_0} \tag{33}$$

Numerical Method

The numerical discretization and solution method, which were provided by Liu et al. [24], are outlined herein for completeness of this work. In order to improve the accuracy of numerical discretization and decrease the discrete points to save computational space, the spectral technique based on the Chebyshev–Gauss–Lobatto points is implemented, which is applied widely for the boundary value problem. The physical grid in the (z, r) domain is transformed into the computational domain (ζ, η) so that the transformed grid lines are orthogonal and suitable for the spectrum method. The domain decomposition method is applied to deal with the singularity of body force at leading and trailing edges. Some transmission conditions are taken into account at the interfaces between the subdomains. The eigenvalue of Eq. (30) is solved numerically over the spectral grids which satisfy

$$\xi_i = \cos(\pi i/N_r); \quad i = 0, 1, \ldots, N_r \tag{34}$$

$$\eta_j = \cos(\pi j/N_z); \quad j = 0, 1, \ldots, N_z \tag{35}$$

where N_r and N_z are the total number of nodes in each subdomain in ζ and η coordinates.

In the present work, the mesh grid in the computation domain is orthogonal and suitable for the spectrum method. In addition, the body force model is utilized to consider the main effects of cascade on the flow field without more flow detail. Such simplification has resulted in a reasonable stability model with high computation efficiency. Body force singularity appears at leading trailing edges because there is no body force in the blade-free region. A singularity typically appears on the leading edge of an airfoil in unsteady flow, and an accurate computation of airfoil flow requires a special treatment of singularities. Rusak and Morris [23] treated the nose singularity for subsonic flow by using matched asymptotic methods of inner solution around the airfoil nose and outer region, which are described by a small disturbance solution. In the present work, the domain decomposition method is applied to deal with the singularity of the body force field. By using the domain decomposition spectral method, different regions (blade region and blade-free region) can be considered to be relatively separate and the mesh can be locally refined. If $f_1(\zeta)$ and $f_2(\zeta)$ are assumed to be two smooth functions of ζ on two subdomains 1 and 2, the continuity conditions for these two functions and their derivatives should be forced on the subdomain domain interface 1_2, i.e.,

$$f_1(\xi_{1\_2}) = f_2(\xi_{1\_2}) \tag{36}$$

$$\frac{df_1(\xi_{1\_2})}{d\xi} = \frac{df_2(\xi_{1\_2})}{d\xi} \tag{37}$$

In Eq. (30), the column vector of perturbation amplitudes $\boldsymbol{\Phi}$ has $K = N_r \cdot (5N_{zf} + 5N_{zb})$ entries, where N_{zf} and N_{zb} are the total number of axial nodes in the blade free and blade row regions, respectively. The $K \times K$ matrix $\boldsymbol{X} = \boldsymbol{A}D_r + \boldsymbol{B}D_z + \boldsymbol{C} - i\omega\boldsymbol{G}$ is very large for a modest number of grid nodes. For instance, there are 20 radial nodes and 50 axial nodes which are spaced 15 upstream, 15 downstream, and 20 in the rotor for a typical single rotor computation, which is a simple case, i.e., $K = 5000$. The matrix $\boldsymbol{X}$ contains 25×10^6 complex value entries. Figure 3 shows the sketch of the entries distribution of matrix $\boldsymbol{X}$, which is a block tridiagonal matrix and the entries of which are zero in the blue region.

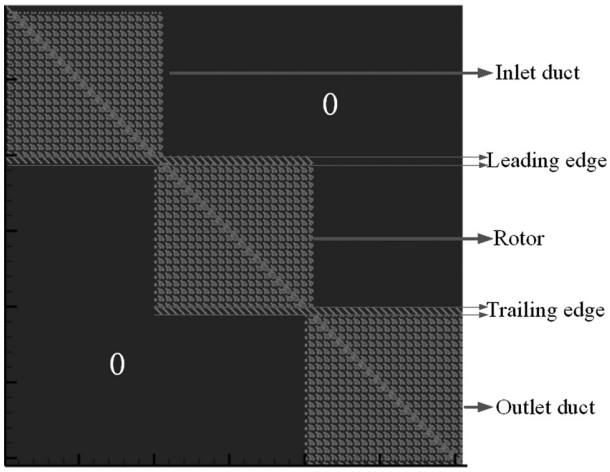

Fig. 3 Sketch of the entries distribution of matrix involved in the established stability equation

It is shown that matrix $\boldsymbol{X}$ will become rather large for multistage compressors and it is not straightforward to solve Eq. (30). Due to the numerical rounding error, it is not feasible to determine the eigenfrequency for which the determinant of $\boldsymbol{X}$ is zero. Solving Eq. (30) is also out of the capability of the traditional QR decomposition method due to accuracy deficiency. These difficulties exist in various stability models, and much research work has been done previously. First, the Newton–Raphson iteration method was widely used to solve the eigenvalue equation. Malik [26] and Gordon [5] implemented an inverse iteration technique to solve the eigenvalue and made progress. However, these two different types of method are very sensitive to the initial estimate of ω and much empiricism is needed to identify pseudomodes. Sun et al. [27] extended the winding number integral approach to solve the matrix equations for the prediction of the rotating stall. The essence of this approach is a smart application of the argument principle and Nyquist stability criterion [28,29]. Nevertheless, it is still not feasible for the problem encountered in the present work because of unsustainable computational time consumption during the determinant calculation process.

In the present investigation, the singular value decomposition (SVD) is adopted over a fine grid on the complex plane to find the solution of Eq. (30). Actually, this approach has been used in many studies [30,31] on finding the roots for which a matrix with many entries becomes singular. As described by Press et al. [32], SVD is a very powerful technique for dealing with the matrices which are either singular or else numerically very close to singular. This method is based on the theorem that any $M \times N$ matrix $\boldsymbol{X}$ can be factorized into a product of a $M \times N$ column-orthogonal matrix $\boldsymbol{U}$, a $N \times N$ diagonal matrix $\boldsymbol{W}$ with positive or zero elements (the singular values), and the transpose of a $N \times N$ orthogonal matrix $\boldsymbol{V}$:

$$\begin{pmatrix} \\ \boldsymbol{X} \\ \\ \end{pmatrix} = \begin{pmatrix} \\ \boldsymbol{U} \\ \\ \end{pmatrix} \bullet \begin{pmatrix} \omega_1 & & \\ & \ddots & \\ & & \omega_N \end{pmatrix} \bullet \begin{pmatrix} \\ \boldsymbol{V}^T \\ \\ \end{pmatrix} \tag{38}$$

Formally, the condition number of a matrix is defined as the ratio of the largest and smallest singular values. A matrix is singular if the condition number is infinite. In other words, the determinant of a matrix is exactly equal to zero only if the reciprocal of the condition number is zero. However, due to the rounding error accumulated during the numerical process, even the machine's floating-point precision is often difficult to be achieved. Cooper et al. [31] defined the roots of the eigenvalue equation as occurring when the reciprocal of the condition number is significantly smaller than elsewhere. In the present work, singular value decomposition (SVD) is adopted over fine grids on the complex plane to find the solution of Eq. (30). Figure 4 shows a result of the reciprocal of condition number by using SVD method on a coarse grid. In this figure, there are five roots with obviously smaller reciprocal of the condition number than elsewhere around them. As long as the grids are extremely refined, we can get the roots of the eigenvalue equation with even more order of magnitude smaller than elsewhere. Obviously, more computational cost is required if the total number of grids are increased. Table 1 compares the accuracy and time consumption of several calculation methods for solving different scale eigenvalue problems. It is shown that the SVD method is an effective technique without sensitivity to initial value for dealing with a large scale matrix equation.

Model Validation on a Transonic Single Stage Compressor

In this section, a model validation is performed to check the applicability of the proposed flow stability model on predicting the stall onset point of a transonic single stage compressor (NASA stage 35) at design rotational speed. NASA stage 35 is an axial-flow inlet stage designed for an eight-stage high-speed compressor. Details of the geometry, blading, and experimental results of this stage were provided by Reid and Moore [33] and Weigl et al. [34]. The main design specifications are displayed in Table 2 and its schematic is shown in Fig. 5.

Figure 6 compares the total-to-static pressure ratio between steady CFD calculation and experimental results provided by Weigl et al. [34]. The steady 3D viscous compressible flow field is computed on a total number of approximate 1.2 and 2.4×10^6 grid nodes, respectively. The calculation results shows that 1.2×10^6 grid nodes are enough to obtain a grid independent result for this single stage with a uniform tip clearance. The solution algorithm is based on central discretization and a four-stage Runge–Kutta scheme coupled with a Spalart–Allmaras turbulence model, multigrid, and local time stepping technique for convergence. The calculated pressure rise is approximate to the experimental data, especially nearby the design point. It is found that the mass flow

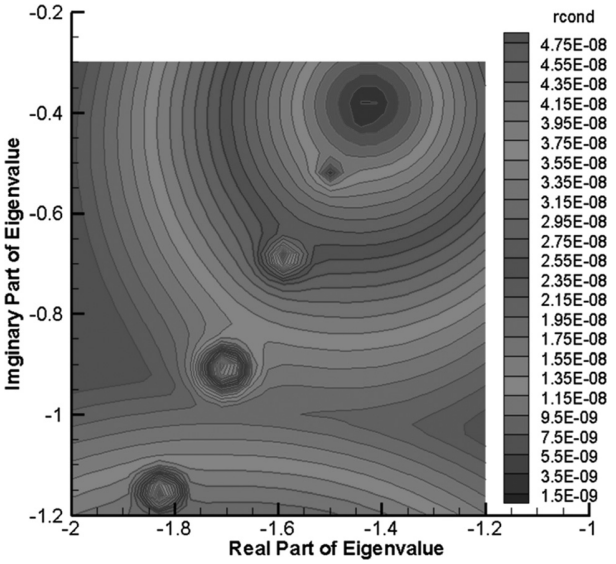

Fig. 4 An example of the contour of the reciprocal number of condition number of matrix *X* on coarse grids of eigenvalue

Table 1 Comparison of several calculation methods (A: computation accuracy; E: computation efficiency)

	Simple equation		Medium scale matrix		Large scale matrix		
	A	E	A	E	A	E	Sensitive to initial value
QR decomposition	√	√	√	√			
Newton–Rapshon iteration	√	√	√				√
Inverse iteration	√	√	√	√			√
Winding number integral	√	√	√	√			
SVD method	√	√	√	√	√	√	

Table 2 Design specifications of stage 35

Design rotational speed (rpm)	17,188.7
Hub–tip ratio	0.7
Rotor aspect ratio	1.19
Stator aspect ratio	1.26
Number of rotor blades	36
Number of stator blades	46

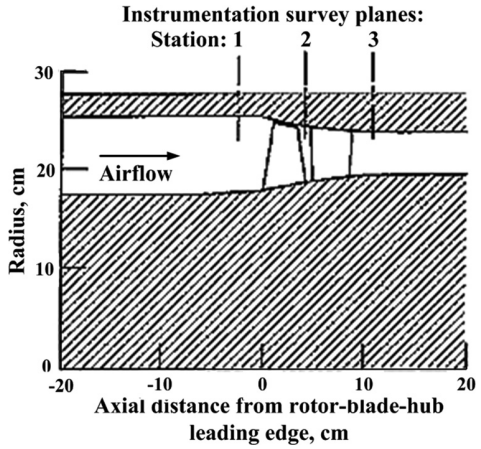

Fig. 5 Schematic of stage 35 (from Reid and Moore [28])

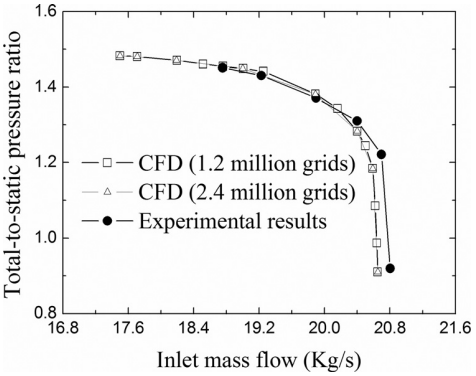

Fig. 6 Total-to-static pressure ratio of stage 35 at design rotational speed

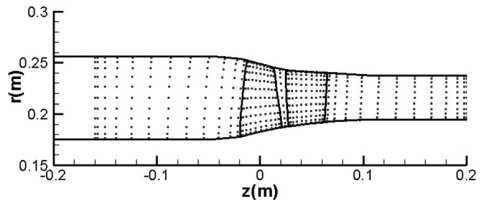

Fig. 7 Distribution of computational grids

at a numerical convergence point is 17.50 kg/s, while the mass flow at the measured stall point is 18.75 kg/s. The relative error is −6.67%, and the stall margin is overpredicted by more than 7%. Obviously, as an unsteady process, rotating stall could not be estimated roughly by the numerical convergence of steady flow simulation.

The discretization nodes, which are shown in Fig. 7, are distributed as 12 radial nodes and 50 axial nodes which are spaced 12 upstream, 12 in the rotor, 3 in the interblade region, 12 in the stator, and 12 downstream. Table 3 shows the convergence of the result of stage 35 with the increased total amount of discretization nodes and it is found that the amount of 12(radial) × 50(axial) discretization nodes is sufficient for a convergent result. There are four subdomains in computational region. It is shown that the density of nodes is locally dense at the hub and tip of the duct and the subdomain interfaces where the flow field variation is strong.

The calculated mean flow data on the meridian plane are processed as polynomial fits of axial and radial coordinates in order to

Table 3 Convergence of the computed eigenvalues of stage 35 at stall inception point using a compressible model

Radial nodes	Axial nodes	RS	DF	Mass flow (kg/s)
8	34	0.75	0.0	18.53
10	42	0.67	0.0	18.80
12	**50**	**0.66**	**0.0**	**18.84**
16	50	0.66	0.0	18.84
16	66	0.66	0.0	18.84

eliminate nonsignificant eigenfrequency due to the local vortex. After the flow field data are introduced into the present model, the complex eigenvalues of the compressor system accompanying the throttling process are computed, which are displayed in Fig. 8. Two eigenmodes within the selected solution interval are obtained for every operation point, which are sequenced as mode 1 and 2 according to the magnitude of the real part. In this assessment, several different values of time delay constant are tested and no visible change of eigenvalue emerges.

It is found that the damping factors of two modes increase gradually as this compressor approaches the flow instability point. The first mode, which propagates rapidly, approaches the instability earlier than the other mode which propagates slowly. The damping factor of mode 1 first changes from negative to positive 18.84 kg/s mass flow. The sign change of the damping factor represents the imminent instability. The relative error of mass flow between the predicted stall inception point and the measured instability point is 0.48%, which is a reasonable prediction of accuracy. While the throttling continues, the relative speed decreases. The propagation speed of this first mode at stall inception is 66% rotational frequency. It is noted that this prediction calculation was conducted on 10 CPU nodes for 12 h, which

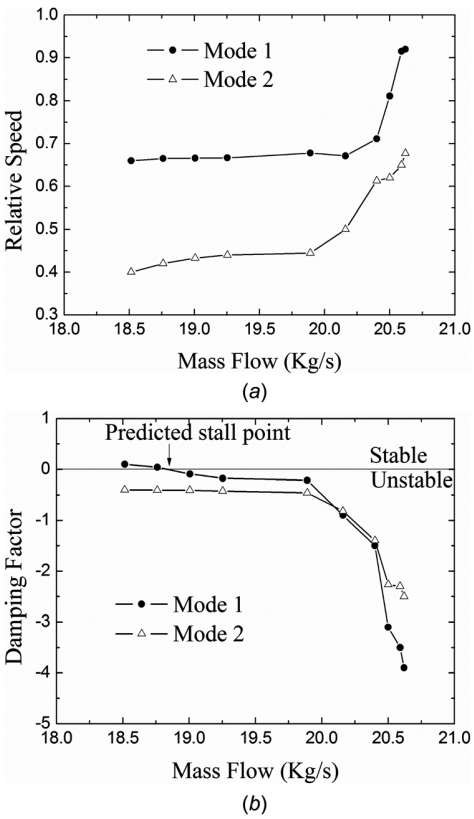

Fig. 8 Computed eigenvalues of stage 35 at design rotational speed: (*a*) Relative speed, and (*b*) damping factor

obviously is a sustainable computational cost for industrial application.

Compressibility Effects on the Stall Onset Point

NASA rotor 37 is a representative transonic single rotor at a design rotational speed, while the spanwise distribution of the inlet relative Mach number ranges from 0.6 to 0.9 at 60% design rotational speed. The details of configuration and characteristics of this rotor were given in a NASA report [35] and detailed experimental data were provided by Suder [36].

Liu et al. [24] computed the stall onset point of this rotor using the compressible flow stability model. It is noted that the present model can be simplified straightly to an incompressible model if the density perturbation is forced to be zero. In this part, the effect of flow perturbation compressibility on the stall onset point is studied by comparing the computed eigenvalues using these two types of models. All the mean flow input data at 60% and 100% rotational speed for the stability model are derived from steady three-dimensional compressible RANS calculation. The details of steady flow calculation and the computed characteristics are given by Liu et al. [24].

Table 4 shows the convergence of the predicted stall onset point of rotor 37 using an incompressible model with the increased total amount of discretization nodes. It is show that the distribution of 12(radial) $\times$ 36(axial) discretization nodes is sufficient for the convergent result. Figure 9 shows the comparison of the computed most unstable eigenvalues using compressible and incompressible flow stability models for rotor 37 at 60% design rotational speed. It is found that the compressible mode becomes unstable at 10.75 kg/s, whereas the damping factor of the incompressible mode crosses the neutral line at 10.89 kg/s. These two mass flow values at the computed stall point are quite close and the relative error is less than 1.4%. However, the compressible unstable mode on the stall inception point propagates at 54.4% rotor speed, while the propagation speed of the incompressible unstable mode is 32.5% rotor speed. The relative error between these two computed values is more than 21%. After crossing the critical line of the system's stability, the damping factors of these two modes rise rapidly. The occurrence of this nonlinear development may be related to the nonlinear feature of the post-stall process of the compressors system. Although this correlation is a conjecture, the most unstable mode predicted by this linear model possibly provides an appropriate initial disturbance for the initial boundary value problem, which aims to study the nonlinear development of the stall precursor. This model assessment reveals that the mass flow at the stall inception point for high subsonic flow seems to be not very sensitive to the compressibility of flow perturbation, but the propagation speed of the stall precursor is indeed accelerated by the flow compressibility.

The following model assessment, which aims to reveal the effect of flow compressibility on transonic flow stability, is conducted on rotor 37 at 100% design rotational speed when the flow field is transonic. After the mean flow data on the meridian plane are introduced into the present stall inception model, the resultant most unstable eigenfrequency using compressible and incompressible at several different operation conditions along the characteristics line is displayed in Fig. 10. It is shown that the damping factor of the compressible and incompressible modes increase

Table 4 Convergence of the computed eigenvalues of rotor 37 at stall inception point using incompressible model

Radial nodes	Axial nodes	RS	DF	Mass flow (kg/s)
8	24	0.41	0.0	10.51
10	30	0.33	0.0	10.80
12	**36**	**0.32**	**0.0**	**10.89**
16	48	0.32	0.0	10.89

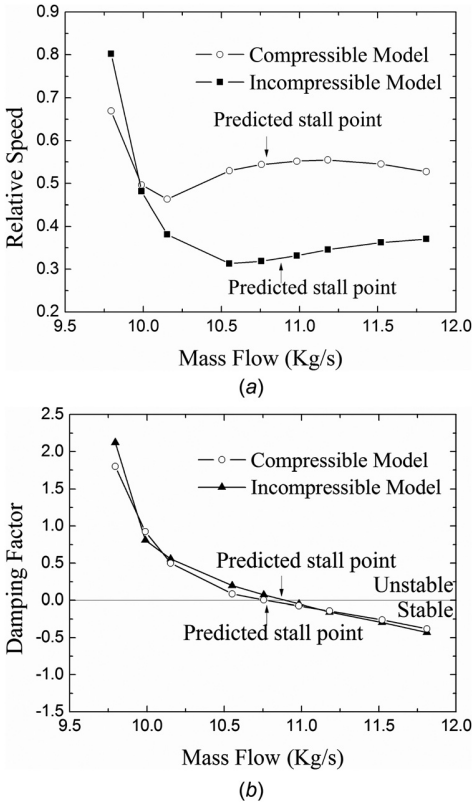

Fig. 9 Computed eigenvalues of rotor 37 at 60% design rotational speed: (*a*) Relative speed, and (*b*) damping factor

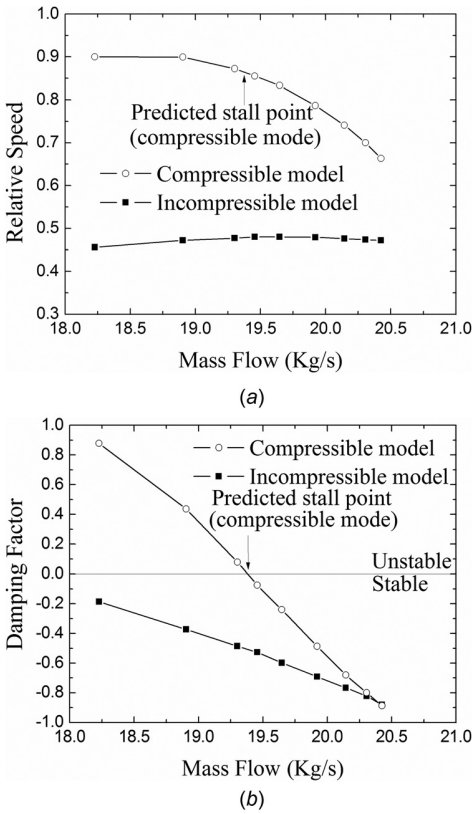

Fig. 10 Computed eigenvalues of rotor 37 at design rotational speed: (*a*) Relative speed, and (*b*) damping factor

linearly as the throttling progressively continues. The compressible mode crosses the critical line when the mass flow decreases to 19.37 kg/s with a relative error of −0.16% compared to 19.4 kg/s which is the measured mass flow at the stall point. However, the computed incompressible mode remains stable until the steady CFD calculation divergence point. The possible unstable point of this mode is roughly estimated to 17.6 kg/s according to the linear interpolation from the resultant eigenvalues, and the relative error compared with the measured stall point is −6.7%. It is obvious that the stall margin is overpredicted inaccurately by the incompressible model and the computed relative speed is also much smaller than that for the compressible model.

Conclusion

In this investigation, the capability of the present model to predict the stall inception point of the high speed single stage axial-flow compressor is validated against the experimental data of NASA stage 35. The compressible stability model for high speed flow is applied for the transonic rotor to investigate the compressibility effects of flow perturbation on the stall onset prediction.

This model is capable of predicting the stall onset point of transonic flow with a relative error of less than 0.5% for the presented model assessment case. It is shown that this stability model could be acceptable for industrial applications during the compressors design phase in terms of sustainable computational source consumption compared with unsteady CFD calculation. In addition, this model can also provide an unambiguous judgment on stall inception without numerous requirements of empirical relations of loss and deviation angle. In industrial practice the stall onset point is generally judged by the convergence of steady CFD calculation, though the stalling process is essentially an unsteady flow phenomenon. The present model could be employed to check the possible overpredicted stall margin caused by steady CFD calculation during the design phase of new advanced transonic compressors without sufficient measurement data.

For the presented transonic rotor, the compressibility mode is the main cause of flow instability inception, whereas the stability of high subsonic flow is not quite sensitive to the flow compressibility and the relative error of flow mass at the stall onset point is less than 1.4%. However, the flow compressibility accelerates the propagation speeds of the stall precursor in both cases by more than 20% for high subsonic flow and more than 30% for transonic flow. It is shown that the compressibility of flow perturbation plays a major role during the stall inception in high speed compressors, especially for transonic flow. Therefore, the flow instability prediction with higher accuracy must be based on the computational model with the effect of flow compressibility.

Acknowledgment

This work is supported by NSFC (Grants No. 51106154, No. 51076006, No. 51010007, and No. 51236001) and 973 Program (Grant No. 2012CB720200).

Nomenclature

$\boldsymbol{A, B, C, G, X}$ = coefficient matrix
c_v = specific heat at constant volume
D_r = radial partial derivative
D_z = axial partial derivative
F = body force scalar
f_θ = unsteady force in circumferential direction
f_z = unsteady force in axial direction
i = imaginary unit
k_c = undetermined body force coefficient
K = dimensionality of matrix
m = circumferential mode number
M, N = integer
n = normal to streamline coordinate in meridian plane
p = static pressure
p_t = stagnation pressure
$\bar{p}_t$ = rotary stagnation pressure
R = gas constant
r_t = radius at the tip of the leading edge
r, θ, z = cylindrical coordinates
T = temperature
t = time
$\boldsymbol{U}$ = column-orthogonal matrix
U_0 = axial velocity of incoming flow at inlet
$\boldsymbol{V}$ = orthogonal matrix
V = velocity scalar
v' = fluctuation velocity scalar
$\vec{\boldsymbol{V}}$ = velocity vector
$\boldsymbol{W}$ = diagonal matrix
β = circumferential metal angle of the mean camber surface in surface (θ, z)
ρ = density
τ = time delay constant
ω = eigenfrequency of the fan/compressors system
ω_r = real part of eigenfrequency
ω_i = imaginary part of eigenfrequency
$\boldsymbol{\Phi}$ = column vector of perturbation amplitudes
Ω = rotational speed of rotor (revolutions per minute)
λ = loss coefficient
ε = body force coefficient
ζ, η = rectangular coordinates in computational plane

Subscripts

a, b = points along one streamline
i, j = integer
t = stagnation property
r, θ, z = radial, circumferential, axial component

Superscript

T = transpose of matrix

References

[1] Emmons, H. W., Pearson, C. E., and Grant, H. P., 1955, "Compressor Surge and Stall Propagation," ASME Trans., **77**(3), pp. 455–469.
[2] Ludwig, G. R., and Nenni, J. P., 1979, "Basic Studies of Rotating Stall in Axial Flow Compressors," AFAPL-TR-79-2083.
[3] Moore, F. K., and Greitzer, E. M., 1986, "A Theory of Post-Stall Transients in Axial Compression Systems," ASME J. Eng. Gas Turbines Power, **108**(1), pp. 68–75.
[4] Stenning, A. H., 1980, "Rotating Stall and Surge," ASME J. Fluids Eng., **102**(1), pp. 14–20.
[5] Gordon, K. A., 1998, "Three-Dimensional Rotating Stall Inception and Effects of Rotating Tip Clearance Asymmetry in Axial Compressors," Ph.D. Thesis, Massachusetts Institute of Technology, Cambridge, MA.
[6] Sun, X. F., 1996, "On the Relation Between the Inception of Rotating Stall and Casing Treatment," 32th AIAA/ASME/SAW/ASEE Joint Conference, Paper No. AIAA-96-2579.
[7] Liu, X. H., Sun, D. K., Sun, X. F., and Wang, X. Y., 2012, "Flow Stability Theory for Fan/Compressors With Annular Duct and Novel Casing Treatment," Chin. J. Aeronaut., **25**(2), pp. 143–154.
[8] Escuret, J. F., and Garnier, V., 1994, "Numerical Simulations of Surge and Rotating Stall in Multi-Stage Axial Flow Compressors," Paper No. AIAA-94-3202.
[9] Longley, J. P., 1997, "Calculating the Flow Field Behaviour of High-Speed Multi-Stage Compressors," ASME Paper No. 97-GT-468.
[10] Chima, R. V., 2006, "A Three-Dimensional Unsteady CFD Model of Compressor Stability," ASME Paper No. GT-2006-90040.
[11] Gong, Y., Tan, C. S., Gordon, K. A., and Greitzer, E. M., 1999, "A Computational Model for Short Wavelength Stall Inception and Development in Multi-Stage Compressors," ASME J. Turbomach., **121**(4), pp. 726–734.
[12] Hoying, D. A., Tan, C. S., Vo, H. D., and Greitzer E. M., 1999, "Role of Blade Passage Flow Structures in Axial Compressor Rotating Stall Inception," ASME J. Turbomach., **121**(4), pp. 735–742.
[13] Vo, H. D., Tan, C. S., and Greitzer, E. M., 2008, "Criteria for Spike Initiated Rotating Stall," ASME J. Turbomach., **130**(1), p. 011023.
[14] Chen, J. P., Hathaway, M. D., and Herrick, G. P., 2008, "Pre-stall Behavior of a Transonic Axial Compressor Stage via Time Accurate Numerical Simulation," ASME J. Turbomach., **130**(4), p. 041014.

[15] Sun, X. F., Liu, X. H., Hou, R. W., and Sun, D. K., 2013, "A General Theory of Flow-Instability Inception in Turbomachinery," AIAA J., **51**(7), pp. 1675–1687.
[16] Tryfonidis, M., Etchevers, O., Paduano, J. D., Epstein, A. H., and Hendricks, G. J., 1995, "Prestall Behavior of Several High-speed Compressors," ASME J. Turbomach., **117**(1), pp. 62–80.
[17] Bonnaure, L. P., 1991, "Modeling High Speed Multistage Compressor Stability," Master Thesis, Massachusetts Institute of Technology, Cambridge, MA.
[18] He, L., 1997, "Computational Study of Rotating-Stall Inception in Axial Compressors," J. Propul. Power, **13**(1), pp. 31–38.
[19] Jacobs, E. N., and Sherman, A., 1937, "Airfoil Section Characteristics as Affected by Variations of the Reynolds Number," NACA TR-586.
[20] Abbott, I. H., and von Doenhoff, A. E., 1959, *Theory of Wing Sections*, 2nd ed., Dover, New York, pp. 124–185.
[21] Rusak, Z., 1993, "Transonic Flow Around the Leading Edge of a Thin Airfoil With a Parabolic Nose," J. Fluid Mech., **248**(1), pp. 1–26.
[22] Morris, W. J., and Rusak, Z., 2013, "Stall Onset on Aerofoils at Low to Moderately High Reynolds Number Flows," J. Fluid Mech., **733**, pp. 439–472.
[23] Rusak, Z., and Morris, W. J., 2011, "Stall Onset on Airfoils at Moderately High Reynolds Number Flows," ASME J. Fluids Eng., **133**(11), p. 111104.
[24] Liu, X. H., Hou, R. W., Sun, D. K., and Sun, X. F., 2012, "Flow Instability Inception Model of Compressors Based on Eigenvalue Theory," 48th AIAA/ASME/SAE/ASEE Joint Propulsion Conference & Exhibit, AIAA-2012-4156, Jul. 30–Aug. 1, Atlanta, GA.
[25] Xu, L., 2003, "Assessing Viscous Body Forces for Unsteady Calculations," ASME J. Turbomach., **125**(3), pp. 425–432.
[26] Malik, M. R., 1982, "Finite-Difference Solution of the Compressible Stability Eigenvalue Problem," Final Report Systems and Applied Sciences Corp., Hampton, VA.
[27] Sun, X. F., Sun, D. K., and Yu, W. W., 2011, "A Model to Predict Stall Inception of Transonic Axial Flow Fan/Compressors," Chin. J. Aeronaut., **24**(6), pp. 687–700.
[28] Brazier-Smith, P. R., and Scott, J. F., 1991, "On the Determination of the Dispersion Equations by Use of Winding Number Integrals," J. Sound Vib., **145**(3), pp. 503–510.
[29] Ivansson, S., and Karasalo, I., 1993, "Computation of Modal Numbers Using an Adaptive Winding-Number Integral Method With Error Control", J. Sound Vib., **161**(1), pp. 173–180.
[30] Woodley, B. M., and Peake, N. 1999, "Resonant Acoustic Frequencies of a Tandem Cascade. Part 1: Zero Relative Motion," J. Fluid Mech., **393**(1), pp. 215–240.
[31] Cooper, A. J., Parry, A. B., and Peake, N., 2004, "Acoustic Resonance in Aero-engine Intake Ducts," ASME J. Turbomach., **126**(3), pp. 432–441.
[32] Press, W. H., Teukolsky, S. A., Vetterling, W. T., and Flannery, B. P., 2001, *Numerical Recipes in Fortran 77: The Art of Scientific Computing*, Cambridge University Press, Cambridge, UK, Chap. 2.
[33] Reid, L., and Moore, R. D., 1978, "Performance of Single-Stage Axial-Flow Transonic Compressor With Rotor and Stator Aspect Ratio of 1.19 and1.26, Respectively, and With Design Pressure Ratio of 1.82," NASA-TP-1338.
[34] Weigl, H. J., Paduano, J. D., Frerchette, L. G., Epstein, A. H., Greitzer, E. M., Bright, M. M., and Strazisar, A. J., 1998, "Active Stabilization of Rotating Stall and Surge in a Transonic Single Stage Axial Compressor," ASME J. Turbomach., **120**(4), pp. 625–636.
[35] Moore, R. D., and Reid, L., 1980, "Performance of Single-Stage Axial-Flow Transonic Compressor With Rotor and Stator Aspect Ratio of 1.19 and1.26, Respectively, and With Design Pressure Ratio of 2.05," NASA-TP-1659.
[36] Suder, K. L., 1997, "Blockage Development in a Transonic, Axial Compressor Rotor," NASA-TM-113115.